Cellular Microbiology (2011) **13**(2), 246–258
doi:10.1111/j.1462-5822.2010.01532.x
First published online 2 November 2010

Role of magnesium and a phagosomal P-type ATPase in intracellular bacterial killing

Emmanuelle Lelong,[1] Anna Marchetti,[1] Aurélie Guého,[2] Wanessa C. Lima,[1] Natascha Sattler,[2] Maëlle Molmeret,[3] Monica Hagedorn,[2†] Thierry Soldati[2] and Pierre Cosson[1*]

[1]*Département de Physiologie Cellulaire et Métabolisme, Faculté de Médecine de Genève, Centre Médical Universitaire, CH1211 Geneva 4, Switzerland.*
[2]*Département de Biochimie, Université de Genève, CH1211 Geneva 4, Switzerland.*
[3]*Université de Lyon1, IFR128, INSERM, U851, Hospices Civils de Lyon, Faculté de Médecine Laënnec, 69007 Lyon, France.*

Summary

Bacterial ingestion and killing by phagocytic cells are essential processes to protect the human body from infectious microorganisms. However, only few proteins implicated in intracellular bacterial killing have been identified to date. We used *Dictyostelium discoideum*, a phagocytic bacterial predator, to study intracellular killing. In a random genetic screen we identified Kil2, a type V P-ATPase as an essential element for efficient intracellular killing of *Klebsiella pneumoniae* bacteria. Interestingly, *kil2* knockout cells still killed efficiently several other species of bacteria, and did not show enhanced susceptibility to *Mycobacterium marinum* intracellular replication. Kil2 is present in the phagosomal membrane, and its structure suggests that it pumps cations into the phagosomal lumen. The killing defect of *kil2* knockout cells was rescued by the addition of magnesium ions, suggesting that Kil2 may function as a magnesium pump. In agreement with this, *kil2* mutant cells exhibited a specific defect for growth at high concentrations of magnesium. Phagosomal protease activity was lower in *kil2* mutant cells than in wild-type cells, a phenotype reversed by the addition of magnesium to the medium. Kil2 may act as a magnesium pump maintaining magnesium concentration in phagosomes, thus ensuring optimal activity of phagosomal proteases and efficient killing of bacteria.

Received 13 August, 2010; revised 22 September, 2010; accepted 24 September, 2010. *For correspondence. E-mail pierre.cosson@unige.ch; Tel. (+41) 22 379 5293; Fax (+41) 22 379 5338.
†Present address: Bernhardt-Nocht Institute for Tropical Medicine, Bernhardt-Noch-strasse 74, 20359 Hamburg, Germany.

Introduction

Phagocytic cells are a key element of the immune system. Monocytes and macrophages ingest and kill microorganisms, thus preventing the development of harmful infections (Segal, 2005). Phagocytosis of large particles (typically > 0.5 μm) relies on the complex interplay of specific receptors at the cell surface, the actin cytoskeleton and actin-binding proteins (Underhill and Ozinsky, 2002). Following uptake, the next stages in the phagocytic process involve notably changes in the protein composition (Garin *et al*., 2001; Haas, 2007) and ionic content (Segal, 2005) of phagosomes (e.g. delivery of lysosomal enzymes and acidification), as well as production of superoxide ions (Sumimoto *et al*., 2005), culminating ultimately with the killing of the ingested microorganisms. The capacity to escape or resist cellular killing mechanisms is a major virulence determinant for many pathogenic bacteria. Therefore, the understanding of cellular killing mechanisms would greatly advance our understanding of host–pathogen interactions.

The mechanisms by which phagocytic cells kill internalized bacteria have been studied intensely in the last decades (reviewed in Segal, 2005; Haas, 2007). Because newly formed phagosomes were observed to progressively acidify and acquire lysosomal enzymes, it was initially proposed that lysosomal enzymes digest and kill bacteria in the acidic environment of phagolysosomes. The discovery of the critical role of the NADPH oxidase in bacterial killing then led to the notion that superoxide and other free radicals were the primary means by which phagocytic cells kill bacteria. More recently, it has been proposed that the main function of NADPH oxidase is to regulate the ionic composition of the phagosome, and to activate lysosomal enzymes (Reeves *et al*., 2002). However, the ionic composition of maturing phagosomes is still poorly characterized to date, as well as the importance of various ions in bacterial killing. It is also not established how many distinct mechanisms exist for

intracellular bacterial killing, and which ones are at play for the killing of various types of bacteria. For both ethical and technical reasons, mammals are not easily amenable to genetic analysis, and no large-scale search for host genes involved in intracellular bacterial killing has been performed so far.

Dictyostelium discoideum amoebae are phagocytic bacterial predators present in the soil. They can be easily grown and manipulated, and their small, haploid, fully sequenced and annotated genome allows simple genetic analysis (Eichinger *et al*., 2005). They have been used extensively to study the structure and dynamics of the endocytic (Neuhaus *et al*., 2002) and phagocytic (Gotthardt *et al*., 2006a) pathways, as well as the intracellular fate of pathogenic bacteria (Cosson and Soldati, 2008). Two *Dictyostelium* mutants defective for intracellular killing of Gram-negative *Klebsiella pneumoniae* bacteria (*phg1a* and *kil1*) have been described (Benghezal *et al*., 2006), suggesting that this model system allows the genetic analysis of intracellular killing mechanisms. Phg1a is a member of the TM9 family of proteins, and Kil1 a sulfotransferase, and the direct or indirect role of these two proteins in bacterial killing remains to be established. In these two mutants, killing defects resulted in an inability to use bacteria as nutrients, suggesting that new killing-defective mutants may be identified by screening for mutants unable to grow on bacteria.

Here we describe the identification, in a random genetic screen, of *Dictyostelium kil2* mutant cells defective for growth on *Klebsiella* bacteria. The *kil2* gene encodes a P-type ATPase essential for intracellular killing of *Klebsiella*. Analysis of *kil2* knockout cells suggests a specific role for magnesium in intracellular killing of *Klebsiella*.

Results

kil2*, an essential gene for growth on* K. pneumoniae

To identify new genes involved in intracellular killing, we performed a random insertional mutagenesis (Guerin and Larochelle, 2002) and selected *Dictyostelium* mutants growing normally in liquid HL5 medium, but defective for growth on a lawn of *Klebsiella* (Fig. 1A). In the *kil2* mutant, the mutagenic plasmid was inserted in the coding sequence of the DDB_G0279183 gene (hereafter named *kil2*), 2121 nucleotides downstream from the start codon (Fig. 1B). To confirm that the selective growth defect of the *kil2* mutant was due exclusively to the disruption of the *kil2* gene, we deleted the *kil2* coding sequence in the wild-type DH1 strain by homologous recombination: 1647 nucleotides were deleted from position 798 to 2445 (Figs 1C and S1). These cells no longer expressed the Kil2 protein (Fig. 1D), exhibited a specific growth defect on *Klebsiella* like the original *kil2* mutant (see below) and were used to further characterize the *kil2* mutant phenotype.

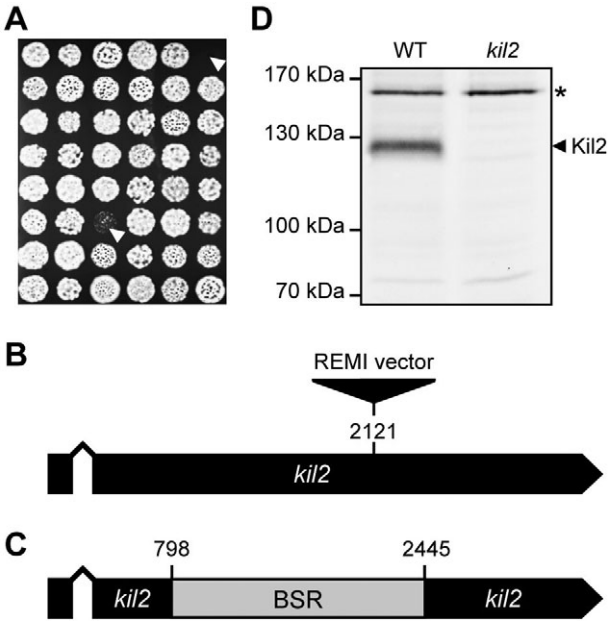

Fig. 1. Isolation of *kil2* mutant cells.
A. *Dictyostelium* mutants were obtained by restriction enzyme mutagenesis insertion and screened for growth on *Klebsiella*. Individual *Dictyostelium* clones were transferred onto a *Klebsiella* lawn (black). Growing *Dictyostelium* cells create phagocytic plaques (white) in the bacterial lawn. In this picture, two *Dictyostelium* clones defective for growth on *Klebsiella* are visible (arrowheads).
B. In the *kil2* restriction enzyme mutagenesis insertion mutant, the mutagenic plasmid was inserted in the coding sequence of DDB_G0279183 gene, 2121 nucleotides downstream from the start codon.
C. The *kil2* knockout mutant was obtained by deleting 1647 nucleotides in the *kil2* coding sequence, and replacing them with a blasticidin-resistance (BSR) cassette.
D. The Kil2 protein is not expressed in *kil2* mutant cells. Arrowhead indicates the Kil2 protein detected by Western blot. The asterisk indicates a non-specific protein recognized by the antiserum.

The predicted Kil2 protein is composed of 1158 amino acid residues, with 10 putative transmembrane domains. It exhibits a strong similarity to members of the P-type ATPase superfamily, which are involved in the active transport of a variety of cations across membranes. The five characteristic domains of P-type ATPases (Catty *et al*., 1997; Axelsen and Palmgren, 1998) are notably conserved in the Kil2 protein (Fig. 2A): the LTGES motif (1) (position 295), the DKTGTLT phosphorylation domain (2) (pos. 467), the ATP binding sites KGA(S)PE (3) (pos. 623) and ML(V)TGD (4) (pos. 717) and the GDGxND hinge sequence (5) (pos. 857). In addition, Kil2 exhibits a PPxxP motif (V) (pos. 424) and two cysteine residues flanking the hinge sequence (Fig. 2B). These two features, as well as a long luminal loop between transmembrane domains 1 and 2 are typical of type V P-ATPases (Figs 2 and S2). Type V family members are only found in eukaryotes, and they form the most poorly characterized family of P-type ATPases (see *Discussion*).

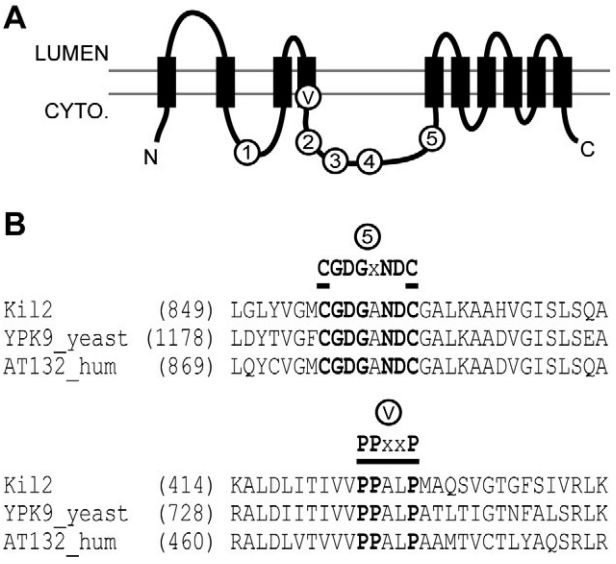

Fig. 2. The Kil2 protein is a type V P-ATPase.
A. The predicted topology of Kil2 shows 10 transmembrane domains. Numbers 1 to 5 indicate the position of the five specific motifs of P-type ATPases: (1) LTGES (2) DKTGTLT (phosphorylation domain) (3) KGA(S)PE and (4) ML(V)TGD (ATP binding sites) (5) GDGxND (hinge sequence). The PPxxP motif specific for type V P-ATPases is also indicated (V).
B. Kil2 presents a high sequence similarity to two type V P-ATPases: yeast YPK9 (YOR291w) and human AT132 (also named ATP13A2). The presence of a PPxxP motif and of two cysteine residues flanking the GDGxND hinge motif is also typical of type V P-ATPases.

In order to characterize the phenotype of *kil2* mutant cells, we tested their ability to grow on a range of bacterial species. For this we applied increasing numbers of *Dictyostelium* cells on a bacterial lawn to monitor quantitatively their ability to form phagocytic plaques (Alibaud *et al*., 2008; Froquet *et al*., 2009) (Fig. 3A). *Kil2* mutants were defective for growth on *Klebsiella*, as well as on a mucoid strain of *Escherichia coli*, but showed no growth defect on many other Gram-negative or Gram-positive bacteria, notably *Bacillus subtilis* or a non-virulent *Pseudomonas aeruginosa* strain (Fig. 3A and B). Interestingly, these results were very similar to those seen with the previously characterized *phg1a* mutant cells (Benghezal *et al*., 2006).

In addition, *kil2* and *phg1a* mutants both grew on a lawn of dead *Klebsiella,* killed either by heat inactivation or by the addition of antibiotics (Fig. 3C). This result suggested that both mutants do not grow on live *Klebsiella* because they are unable to kill these bacteria efficiently.

Kil2 is essential for efficient intracellular killing of Klebsiella

Defective growth on bacteria could conceivably be due to defects in bacterial ingestion, in bacterial killing or in a range of other cellular functions. Phagocytosis of *Klebsiella* and of latex beads was unaffected in *kil2* mutant cells compared with wild-type cells (Fig. 4A) ruling out the possibility that the *kil2* growth defect might be due to decreased bacterial internalization. In order to assess if

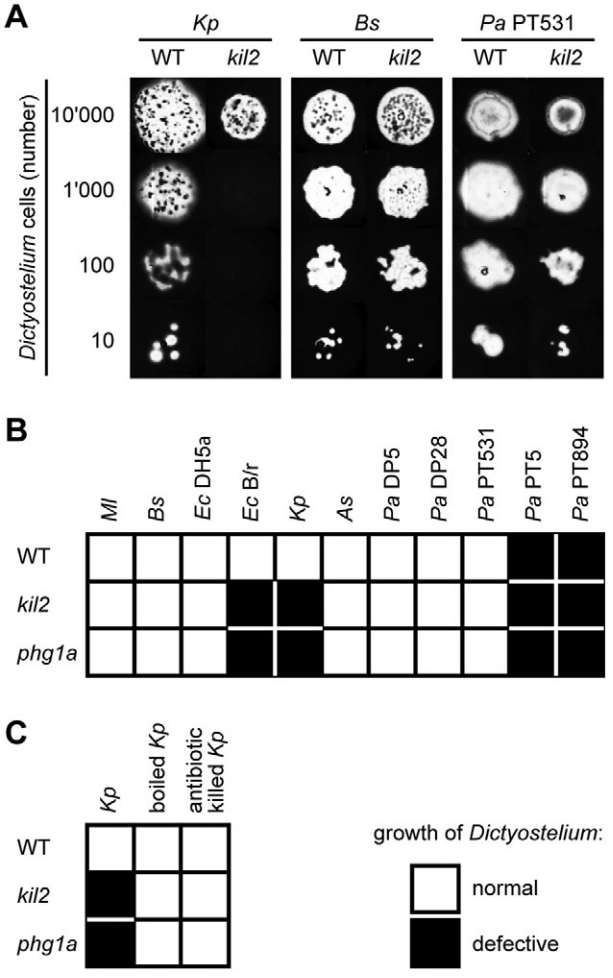

Fig. 3. *kil2* mutant cells are specifically defective for growth on *Klebsiella*.
A. In order to quantify the ability of *Dictyostelium* strains to grow on bacteria, 10 000, 1000, 100 or 10 *Dictyostelium* cells were applied onto a bacterial lawn (black). Wild-type *Dictyostelium* cells created a phagocytic plaque (white). *kil2* cells grew normally on *B. subtilis* and on avirulent *P. aeruginosa* but presented an important growth defect on *Klebsiella*.
B. Growth of *kil2* cells on several bacterial species was tested as described in A. Normal growth of *Dictyostelium* cells is indicated in white, defective growth in black. Wild-type *Dictyostelium* grew on a collection of Gram-negative and Gram-positive bacteria and did not grow on virulent bacteria like wild-type *P. aeruginosa*. The *kil2* and *phg1a* mutants exhibited the same specific growth defects on *Klebsiella* and on the mucoid *E. coli* B/r strain. (*As: Aeromonas salmonicida, Bs: Bacillus subtilis, Ec: Escherichia coli, Kp: Klebsiella pneumoniae, Ml: Micrococcus luteus, Pa: Pseudomonas aeruginosa*.)
C. Normal growth of *kil2* and *phg1a* cells was restored when *Klebsiella* were boiled before the growth test or deposited on SM-agar containing antibiotic (gentamycin 25 μg ml^{-1}).

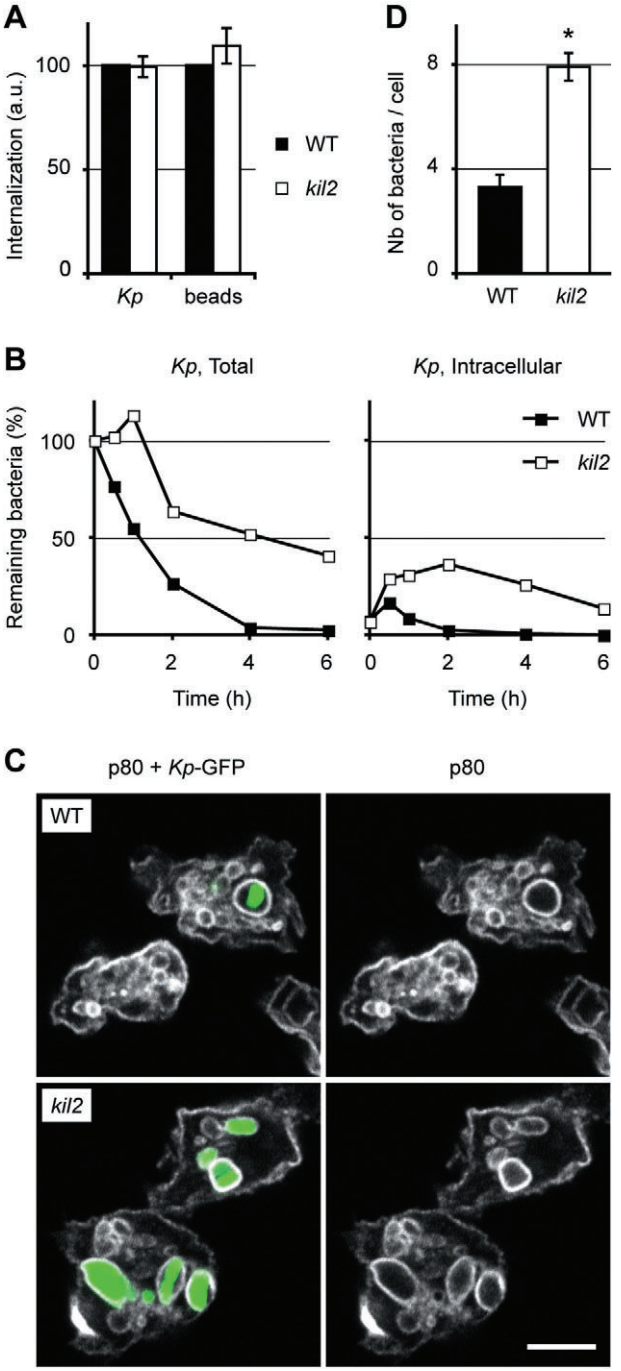

Fig. 4. Inefficient intracellular killing of *Klebsiella* in *kil2* mutant cells.
A. Phagocytosis is not defective in *kil2* mutant cells. Wild-type or *kil2* cells were incubated with fluorescent latex beads or fluorescently labelled *Klebsiella* for 20 min. The cells were then washed and the internalized fluorescence measured by flow cytometry. The average and SEM of six independent experiments are indicated.
B. *Dictyostelium* cells were incubated with *Klebsiella* and the number of surviving bacteria (total or cell-associated) was determined at different times by killing the *Dictyostelium* and plating the bacteria on LB plates. Wild-type *Dictyostelium* cells killed *Klebsiella* rapidly and very few viable cell-associated bacteria were detected. On the contrary, *kil2* mutant cells killed *Klebsiella* inefficiently and a significant number of live intracellular bacteria were detected in these cells. This experiment was repeated four times with equivalent results.
C. *Dictyostelium* cells were incubated in the presence of *Klebsiella*-GFP for 90 min, and then fixed. The endosomal p80 marker was revealed by immunofluorescence (white) and cells observed by confocal microscopy. Live fluorescent *Klebsiella* (green) were always observed inside p80-positive compartments and accumulated more prominently in *kil2* mutant cells (scale bar: 5 μm).
D. In cells analysed as described in C, the number of fluorescent bacteria was quantified within 100 cells. Each bar indicates the average and SEM of five independent experiments. The statistical significance of these results was established using the Student's *t*-test (*$P < 0.001$).

kil2 cells killed efficiently bacteria, live *Klebsiella* were incubated with *Dictyostelium* cells for up to 6 h. At 0, 1, 2, 4 and 6 h, the total number of remaining viable bacteria was determined, as well as the number of live cell-associated bacteria. Wild-type *Dictyostelium* ingested and killed bacteria rapidly (Fig. 4B). Intracellular killing in wild-type cells was so fast that viable intracellular bacteria were hardly detectable at any time, suggesting that under these experimental conditions the limiting factor for killing was the rate of phagocytosis. On the contrary, *kil2* mutant cells killed *Klebsiella* slowly, and live intracellular bacteria accumulated in these cells (Fig. 4B).

The fluorescence of GFP-expressing bacteria disappears rapidly when they are killed (Benghezal *et al*., 2006). Therefore, to visualize the intracellular killing activity, we incubated GFP-expressing *Klebsiella* with *Dictyostelium* cells for 90 min. Cells were then fixed and endosomal compartments visualized by immunofluorescence using a monoclonal antibody to endosomal p80 (Ravanel *et al*., 2001). In both wild-type and *kil2* mutant cells, live fluorescent bacteria were always observed in phagosomal compartments delimited by a p80-positive membrane (Ravanel *et al*., 2001) (Fig. 4C). However, two times more fluorescent bacteria accumulated within *kil2* mutant cells than within wild-type cells (Fig. 4C and D). This result further suggested that intracellular killing of *Klebsiella* was inhibited in *kil2* mutant cells.

In order to assess the specificity of the killing defect observed in *kil2* mutant cells, we tested the ability of these cells to kill other bacterial strains. Like *phg1a* mutant cells, *kil2* mutants killed *Klebsiella* more slowly than wild-type cells did, but showed no defect in killing of *B. subtilis* and *P. aeruginosa* (Fig. 5A). This result is in agreement with the observation that *kil2* mutant cells grew readily on the latter two bacteria, and confirmed the specificity of the *kil2* killing defect for *Klebsiella*.

In a previous study, *Klebsiella* mutants were selected based on their ability to support growth of killing-defective *phg1a* mutant cells (Benghezal *et al*., 2006). Two of these

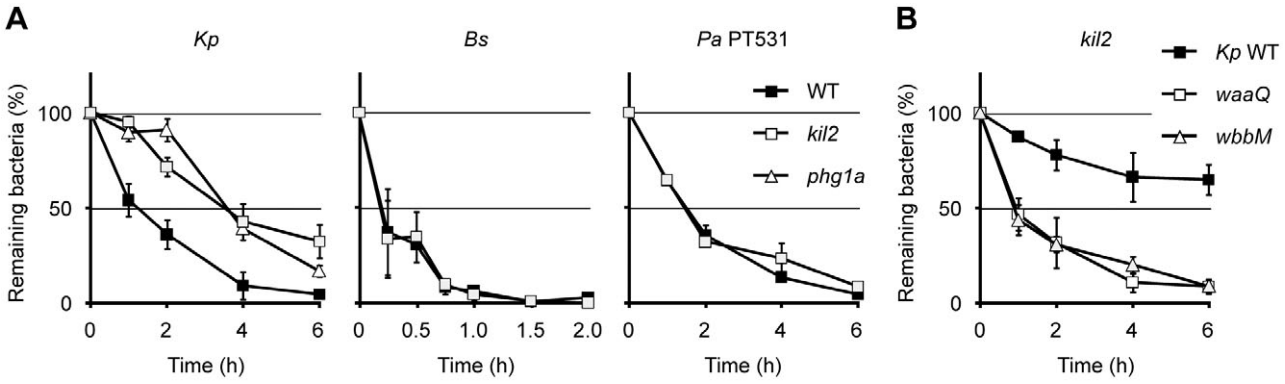

Fig. 5. The killing defect of *kil2* mutant cells is specific for certain bacterial species. *Dictyostelium* cells were incubated with *Klebsiella* (*Kp*), *B. subtilis* (*Bs*) or avirulent *P. aeruginosa* (*Pa* PT531) and the total number of viable bacteria was determined at the indicated times as described in the legend to Fig. 4. The mean and SEM of three independent experiments are shown.
A. *kil2* mutant cells killed inefficiently *Klebsiella*, but normally *B. subtilis* and *P. aeruginosa*. A similar phenotype was observed in *phg1a* mutant cells.
B. *kil2* mutant cells killed efficiently *Klebsiella* mutants with altered surface biosynthesis (*waaQ* and *wbbM*).

Klebsiella strains were mutated in genes involved in the biosynthesis of the bacterial cell wall (*waaQ* and *wbbM*), and they were more easily killed by *phg1a* mutant cells than wild-type *Klebsiella*. Interestingly, these two *Klebsiella* strains were also more easily killed by *kil2* mutant cells (Fig. 5B), further reinforcing the resemblance between the phenotypes of *phg1a* and *kil2* mutants. This result strongly suggests that the particular composition of the *Klebsiella* surface allows them to withstand killing by *kil2* and *phg1a* mutant cells.

The killing defect exhibited by *kil2* knockout cells could be due to a gross defect in the organization and/or dynamics of the endocytic/phagocytic pathway. Therefore, we assessed several key parameters of the endocytic/phagocytic pathway. Macropinocytosis of fluid phase containing a fluorescent dextran was measured by flow cytometry, and was as efficient in *kil2* cells as in wild-type cells (110.27% $\pm$ 5.83; $n = 3$). The pH of lysosomal and post-lysosomal compartments, as well as the speed at which ingested fluid phase was transferred from acidic lysosomes to more neutral post-lysosomes was identical in wild-type and *kil2* cells (Fig. S3). Quantitative immunofluorescence analysis during phagocytosis of latex beads revealed that the residency time of beads in lysosomes (p80-positive, H^+-ATPase-positive) before their transfer to post-lysosomes (p80-positive, H^+-ATPase-negative) was also very similar in wild-type and *kil2* mutant cells (Fig. S4A). The activity of several lysosomal enzymes was virtually identical in wild-type and *kil2* knockout cells (Fig. S4B). Finally, the size and numbers of lysosomes and post-lysosomes were determined after immunofluorescence staining, and were very similar in both cell types (Table S1). Overall, these results show that the killing defect of *kil2* mutants is not accompanied by a strong alteration in the general organization or dynamics of the endocytic/phagocytic pathway.

Co-purification of Kil2 with phagosomal membranes

Because our results implicated the Kil2 protein in bacterial killing, we hypothesized that Kil2 localizes to phagosomes, the organelle in which killing is achieved. To test this hypothesis, we allowed *Dictyostelium* cells to phagocytose latex beads, and purified on a sucrose gradient latex beads containing phagosomes at various stages of maturation (Gotthardt *et al*., 2006b; Dieckmann *et al*., 2008). We then used specific antibodies to assess the protein content of phagosomes. Kil2 was readily detectable in early phagosomes, and accumulated further in maturing phagosomes (Fig. 6), a profile resembling that of

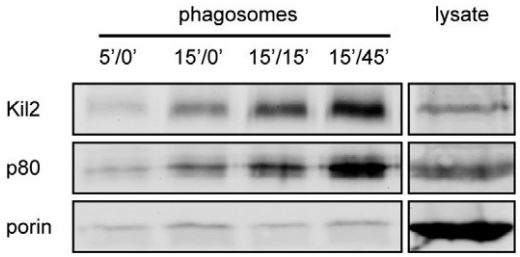

Fig. 6. Co-purification of the Kil2 protein with phagosomes. Cells were incubated with latex beads during 5 or 15 min, washed to eliminate non-internalized beads and incubated further for 15 or 45 min, as indicated. Phagosomes containing latex beads were purified on sucrose gradients and analysed by Western blot in order to detect the presence of different proteins: Kil2, endosomal p80 and mitochondrial porin. Kil2 was detectable in very early phagosomes and gradually accumulated during the maturation of phagosomes. This pattern was extremely similar to that of endosomal p80. Only trace amounts of mitochondrial porin were detected in phagosomal fractions.

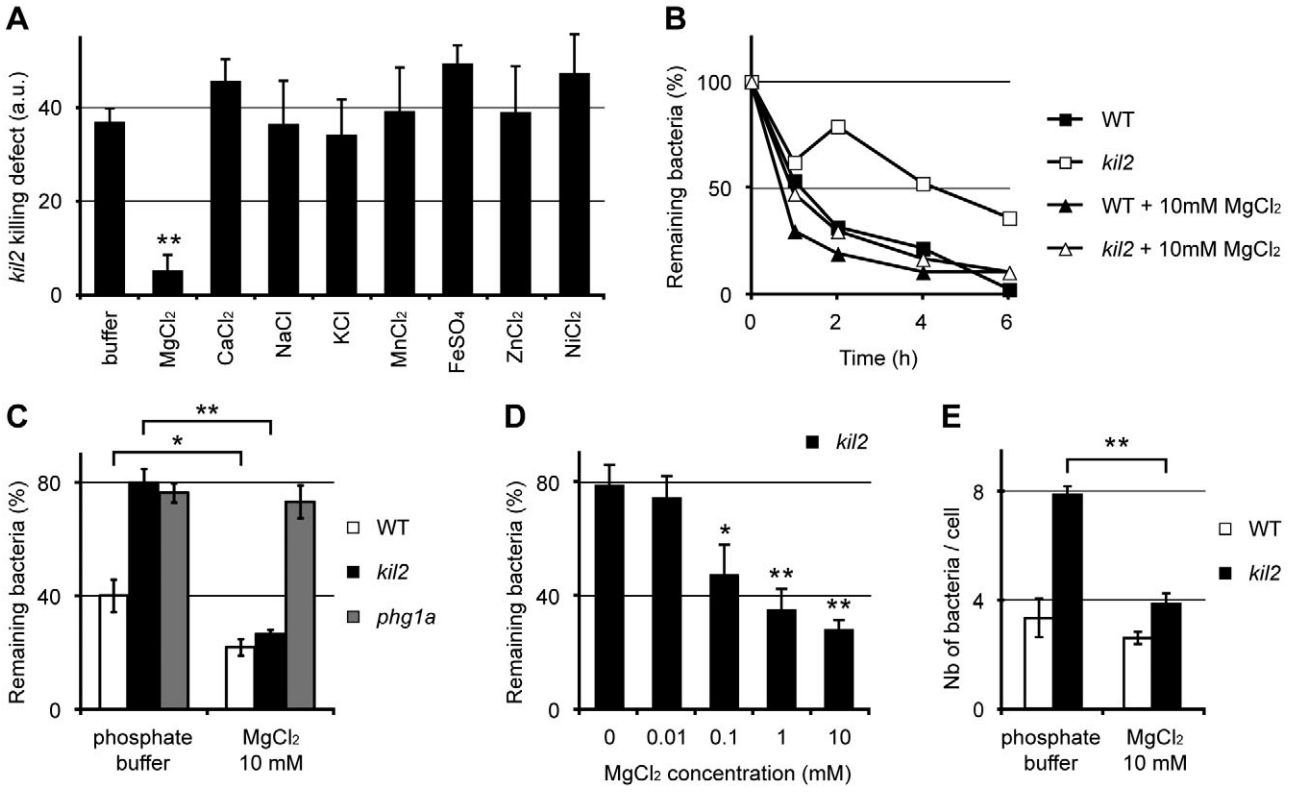

Fig. 7. Exogenous magnesium restores efficient killing in *kil2* mutant cells.
A. Intracellular bacterial killing was assessed as described in the legend to Fig. 5, but with one of the following salts added to the extracellular medium: $MgCl_2$ (10 mM), $CaCl_2$ (10 mM), NaCl (10 mM), KCl (10 mM), $MnCl_2$ (10 μM), $FeSO_4$ (10 μM), $ZnCl_2$ (1 μM), $NiCl_2$ (0.5 μM). The *kil2* killing defect is the difference between the percentages of remaining bacteria in wild-type and *kil2* cells, after 2 h of incubation. Exogenous magnesium was the only ion abolishing the killing defect of *kil2* mutant cells.
B. A typical killing experiment, showing the killing of *Klebsiella* by wild-type or *kil2* knockout cells in the presence or absence of extracellular $MgCl_2$. In the presence of 10 mM $MgCl_2$, efficient killing of *Klebsiella* by *kil2* mutant cells was restored.
C. The percentage of remaining live bacteria after 2 h is shown for wild-type, *kil2* and *phg1a* cells. Addition of 10 mM $MgCl_2$ in the medium restored the killing capacity of *kil2* mutant cells whereas *phg1a* mutant cells were still unable to kill *Klebsiella* efficiently. It also slightly accelerated killing in wild-type cells.
D. Killing was assessed as described above but in the presence of increasing concentrations of $MgCl_2$ (0.01, 0.1, 1 or 10 mM). The effect of exogenous $MgCl_2$ on intracellular killing was dose-dependent and visible at concentrations above 100 μM.
E. Wild-type or *kil2* mutant cells were incubated with GFP-expressing *Klebsiella* for 90 min. The cells were then fixed, and the number of intracellular fluorescent bacteria was determined as described in the legend to Fig. 4. The intracellular accumulation of live bacteria in *kil2* cells was abolished by the addition of 10 mM $MgCl_2$ in the medium.
All experiments were repeated at least three times (average and SEM are indicated). The statistical significance of the results was determined using the Student's *t*-test (*$P < 0.05$ and **$P < 0.01$).

the p80 endosomal marker (Fig. 6). Mitochondrial porin was virtually absent from phagosomal preparations (Fig. 6). The presence of Kil2 in purified phagosomal membranes suggests that it may participate in creating an appropriate environment for efficient intracellular killing of ingested *Klebsiella*.

A role for magnesium in bacterial killing

Assuming that Kil2 pumps a specific cation into the phagosomal lumen that is essential for *Klebsiella* killing, then providing this ion in the extracellular medium may restore its intra-phagosomal concentration and consequently efficient killing in *kil2* mutant cells. A similar strategy has been used previously to determine the ability of various ions to induce expression of bacterial genes within phagosomes (Martin-Orozco *et al*., 2006). However, this approach is limited by the fact that certain ions have toxic or inhibitory effects on cells. We thus tested the effect of each ion at the highest concentration at which it did not inhibit killing of *Klebsiella* by wild-type *Dictyostelium*. Extracellular addition of $CaCl_2$ (10 mM), NaCl (10 mM), KCl (10 mM), $MnCl_2$ (10 μM), $FeSO_4$ (10 μM), $ZnCl_2$ (1 μM) or $NiCl_2$ (0.5 μM) did not increase killing of *Klebsiella* in *kil2* cells (Fig. 7A). However, efficient killing was restored in *kil2* cells by the extracellular addition of $MgCl_2$ (10 mM) (Fig. 7A). In the presence of magnesium, *kil2* mutant cells killed *Klebsiella* as rapidly as wild-type cells (Fig. 7B).

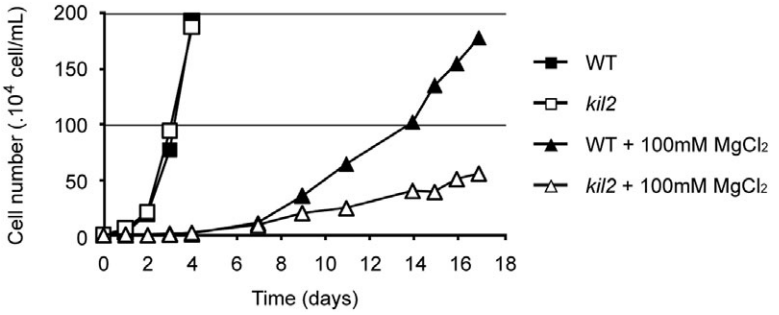

Fig. 8. *kil2* knockout cells are sensitive to high magnesium concentrations. Growth of wild-type and *kil2* mutant cells was tested in HL5 medium supplemented or not with 100 mM $MgCl_2$. In HL5, *kil2* knockout cells grew as well as wild-type cells. In the presence of 100 mM $MgCl_2$, *kil2* cells grew more slowly than wild-type cells. This experiment was reproduced three times with similar results.

Remarkably, addition of extracellular magnesium had no effect on the killing defect of *phg1a* mutant cells (Fig. 7C). This contrasting behaviour rules out the possibility that the observed effect was due to a non-specific toxic effect of magnesium on bacteria. The effect of magnesium on the killing ability of *kil2* cells was dose-dependent, and detectable at concentrations above 100 μM (Fig. 7D). This result was also confirmed by measuring intracellular accumulation of live *Klebsiella*-GFP: in the presence of 10 mM $MgCl_2$, *kil2* cells no longer accumulated high numbers of undigested intracellular bacteria (Fig. 7E).

The ionic specificity of a P-type ATPase can also be determined by measuring the ability of a mutant strain to grow when exposed to very high concentrations of various ions (Schmidt *et al.*, 2009). For this we used ionic concentrations that slowed down significantly but not completely growth of wild-type *Dictyostelium* cells. Mutant *kil2* cells grew as well as wild-type cells in HL5 medium, but significantly more slowly in a medium supplemented with 100 mM $MgCl_2$ (Fig. 8). No significant difference between wild-type and *kil2* cells were observed when cells were grown in medium supplemented with KCl (200 mM), NaCl (150 mM), $CaCl_2$ (80 mM), $MnCl_2$ (15 mM), $CdCl_2$ (50 μM) or $NiCl_2$ (350 μM) (data not shown). These observations suggest that Kil2 may participate in sequestration of magnesium ions in endosomal compartments.

In order to understand how phagosomal magnesium may influence bacterial killing, we measured in living cells the activity of phagosomal proteases. For this, latex beads coupled to fluorescently labelled BSA were fed to amoeba, and the fluorescence recorded as a function of time. The fluorescence attached to the beads is quenched, but increases when it is released from the beads upon proteolysis of BSA (see *Experimental procedures*). This assay revealed that phagosomal protease activity was significantly lower in *kil2* knockout cells than in wild-type cells (Fig. 9A), a defect fully compensated by the addition of magnesium in the medium (Fig. 9B). This result suggests that Kil2 controls the activity of phagosomal proteases by maintaining an appropriate magnesium concentration in phagosomes.

Kil2 is not implicated in intracellular bacterial replication

In addition to its role in bacterial killing, the ionic composition of phagosomes is also a key determinant in the intracellular replication of some bacterial pathogens. This has been established particularly clearly by studying cells defective for the function of Nramp1, a putative phagosomal iron transporter. The lack of activity of Nramp1 (natural resistance-associated macrophage protein) renders mammalian phagocytic cells more susceptible to intracellular replication of several different intracellular pathogens, notably *Salmonella*, mycobacteria and *Leishmania* (reviewed in Papp-Wallace and Maguire, 2006). In *Dictyostelium*, intracellular replication of mycobacteria and of *Legionella* is facilitated in *nramp1* knockout cells

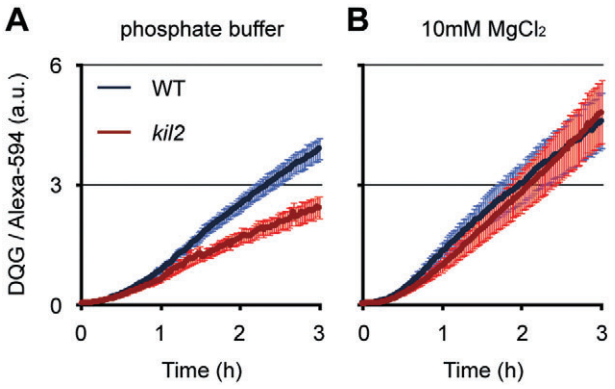

Fig. 9. Phagosomal proteolysis is defective in *kil2* mutant cells, but restored by exogeneous magnesium. Wild-type or *kil2* mutant cells were incubated with latex beads coupled to fluorescent BSA. Fluorescence is quenched at the surface of beads, but increases when the fluorophore is released in the lumen upon digestion of BSA.
A. In phosphate buffer, protease activity was lower in *kil2* mutant cells than in wild-type cells.
B. Addition of 10 mM MgCl2 to the phosphate buffer restored normal protease activity in *kil2* mutant cells. The curves represent the average and SEM of 13 independent measures in 6 independent experiments. The values attained after 3 h were significantly different for wild-type and *kil2* mutant cells in phosphate buffer ($P < 0.01$; Student's *t*-test), but not in buffer supplemented with 10 mM MgCl2 ($P > 0.25$). The protease activity was also not significantly different in wild-type cells incubated in phosphate buffer or in magnesium-enriched buffer ($P > 0.25$).

(Peracino *et al*., 2006). To determine if *nramp1* and *kil2* mutant cells present similar phenotypes, we investigated first if intracellular replication of bacteria was facilitated in *kil2* cells, and second if intracellular killing of *Klebsiella* was inhibited in *nramp1* cells.

Dictyostelium is an established host model for pathogenic *Mycobacterium marinum*, and the replication of GFP-expressing *M. marinum* can be visualized and quantified with precision (Hagedorn and Soldati, 2007). During infection of wild-type cells, internalized *M. marinum* are found in a p80-positive replication compartment, from which they eventually escape to the cytosol. The replication niche of *M. marinum* was indistinguishable in wild-type and *kil2* cells, and accumulation of p80, as well as vacuole rupture were frequently observed (Fig. S5A). Flow cytometry analysis of infected cells also revealed a virtually identical rate of intracellular replication in wild-type and mutant cells (Fig. S5B). Finally, an avirulent *M. marinum* mutant (L1D) was unable to replicate in *kil2* mutant cells as well as in wild-type cells (Fig. S5B). These results indicate that the Kil2 protein is not involved in intracellular replication of *M. marinum* in *Dictyostelium* cells, neither as a limiting factor, nor as a facilitating element.

Conversely, we did not observe any defect in the ability of *nramp1* mutant cells to kill *Klebsiella* compared with wild-type cells (Fig. S6), indicating that Nramp1 does not play a critical role in intracellular killing of *Klebsiella* in *Dictyostelium*. Together, these results suggest that different host mechanisms are involved in intracellular killing of *Klebsiella* and during intracellular replication of *M. marinum*.

Discussion

In this study we identified in a random genetic screen Kil2, a new gene product involved in intra-phagosomal killing of *Klebsiella* in *Dictyostelium*. In *kil2* knockout cells, the overall organization of the endocytic pathway is essentially unaffected, but intra-phagosomal killing of *Klebsiella* is very inefficient. Kil2 exhibits all the sequence characteristics of a type V P-ATPase and is present in the phagosomal membrane, it may thus be expected to pump cations into the phagosomal lumen. Efficient killing was restored in *kil2* mutant cells when magnesium ions were added to the extracellular medium together with the bacteria, presumably restoring an adequate magnesium concentration in phagosomal compartments. The simplest interpretation of our results is that Kil2 transports magnesium into the phagosome, and that magnesium is required for optimal protease activity and efficient intracellular killing of *Klebsiella*.

Not much is known about type V P-ATPases. Although it is assumed that, like most other P-type ATPases, they are cation pumps, their substrate specificity is not established with certainty (Axelsen and Palmgren, 1998; Schultheis *et al*., 2004). In human, mutations in ATP13A2, a lysosomal member of the family, are responsible for a hereditary form of Parkinsonism, but the cellular function of ATP13A2 is unclear (Ramirez *et al*., 2006). At the cellular level, type V P-ATPases were mostly studied in *Saccharomyces cerevisiae*. In this organism, there are 16 P-type ATPases (Catty *et al*., 1997), two of which belong to the type V: Cod1/Spf1/YEL031w and Ypk9p. Ypk9 has been localized to the vacuole, and its absence renders cells more sensitive to heavy metal ions (e.g. Cd^{2+} and Ni^{2+}), suggesting that it may sequester these ions in the vacuole (Gitler *et al*., 2009; Schmidt *et al*., 2009). Cod1 plays a role in the ionic homeostasis of the ER, and its loss leads notably to alterations of the secretory pathway (e.g. protein stability, glycosylation) (Cronin *et al*., 2002). Interestingly, there are indications that Cod1 may transport magnesium ions (Cronin *et al*., 2002). Indeed magnesium was the only ion capable of stimulating Cod1p ATPase activity *in vitro*. The effect was seen at relatively high concentrations (1 to 10 mM, i.e. 200 times more than the ATP concentration), suggesting that it could not be attributed to ATP-bound magnesium ions (Cronin *et al*., 2002). In summary, although the ion specificity of type V P-ATPases remains to be firmly established, they may be involved in the transport of heavy metal ions, and of magnesium. Our results reinforce the notion that at least some type V P-ATPases may act as magnesium transporters.

The role of magnesium in bacterial survival within phagosomes has been a debated subject, particularly its role in intracellular replication of *Salmonella*. It was initially observed that magnesium depletion *in vitro* induces the expression of several *Salmonella* genes essential for replication within phagosomes, notably *phoPQ* (Garcia Vescovi *et al*., 1996). Another gene, *mgtC*, was shown to be essential for growth of *Salmonella* in magnesium-depleted medium *in vitro*, as well as in phagosomes (Alix and Blanc-Potard, 2007). These observations led to the idea that bacteria encounter conditions of magnesium depletion in phagosomes. This was proposed to be part of a general cellular strategy aimed at depriving internalized bacteria of nutrients, in order to control their replication and to facilitate their killing (Appelberg, 2006). However, it was later shown that phagosomal acidification, and not magnesium depletion, may be the critical element inducing PhoPQ in phagosomes (Martin-Orozco *et al*., 2006). Other studies also suggested that the two functions of MgtC (growth in magnesium-deprived medium and intracellular replication) can be dissociated (Alix and Blanc-Potard, 2007). Finally, direct measurement revealed a stable concentration of magnesium (approximately 1 mM) in phagosomes (Martin-Orozco *et al*., 2006), suggesting

the existence of a mechanism actively maintaining magnesium concentration in this compartment. Our results extend this notion one step further: they suggest that the presence of magnesium in phagosomes is not beneficial to all internalized bacteria, and is actually critical to achieve efficient killing of internalized *Klebsiella.* Our results suggest that a minimal concentration of magnesium may be necessary for optimal activity of phagosomal enzymes (e.g. proteases). Exogenous magnesium even stimulates the killing of Klebsiella by wild-type cells, maybe because an optimal phagosomal magnesium concentration is more readily attained in these conditions. While the simplest interpretation of our results would be that Kil2 itself is a magnesium transporter, there are a number of alternative interpretations. One possibility is that Kil2 participates only indirectly in magnesium homeostasis in phagosomes, for example, if its activity is coupled to that of other magnesium-specific channels. Another scenario is that there may be several redundant killing mechanisms, one Kil2-dependent, the other magnesium-dependent. Magnesium would then only be necessary for killing when the Kil2-dependent killing is inactivated, i.e. in *kil2* but not in wild-type cells.

From a more general perspective, our results confirm previous observations suggesting that the killing of *Klebsiella* mobilizes a specific set of gene products, which is not essential for the killing of other types of bacteria (e.g. *B. subtilis* or *P. aeruginosa*). Indeed the growth and killing defects of *kil2* mutant cells are very similar to those observed for *phg1a* and *kil1* mutant cells previously (Benghezal *et al*., 2006), and are restricted to a small subset of Gram-negative bacteria (*Klebsiella* and a mucoid *E. coli* isolate). This subset of bacteria is most likely defined by specific bacterial surface determinants, as suggested by the fact that *kil2* and *phg1a* mutant cells kill readily *Klebsiella* mutants with defective cell wall synthesis. This result stresses the importance of the nature of the bacterial surface in determining resistance to specific killing mechanisms. Intracellular replication of mycobacteria is not affected in *kil2* mutant cells, suggesting that Kil2 is involved neither in limiting mycobacterial replication, nor in facilitating it. Conversely, we observed that Nramp1, which inhibits replication of mycobacteria (Peracino *et al*., 2006), was dispensable for efficient killing of *Klebsiella*. Overall, these results indicate that distinct host mechanisms are involved in the killing of different types of bacteria, and in limiting the replication of pathogens. An extensive genetic analysis will be necessary to determine the mechanisms involved in the intracellular killing or survival of various types of bacteria. In this perspective, *Dictyostelium* amoebae are attractive model phagocytic cells, as they are amenable to genetic analysis, and their interactions with bacteria can be studied relatively easily.

Experimental procedures

Cells and reagents

Unless otherwise specified, all mutant *Dictyostelium* strains used in this study were derived directly from the subclone DH1-10 (Cornillon *et al*., 2000) of the DH1 strain (Caterina *et al*., 1994), referred to here as wild-type for simplicity. The *phg1a* mutant was described previously (Cornillon *et al*., 2000). The *nramp1* mutant and the corresponding AX2 parental strain were a kind gift of Dr S. Bozzaro (University of Turin, Italy) (Peracino *et al*., 2006).

A polyclonal antibody recognizing the Kil2 protein was obtained by immunization of rabbit (Covalab, France) with two peptides corresponding to sequences in the C-terminal portion of Kil2: KSKRKLKQKQNSDP and IIAKNTVNERYTSLN. The H161 monoclonal antibody recognizing the p80 endosomal protein and the monoclonal antibody 70-100-1 recognizing the mitochondrial porin were described earlier (Troll *et al*., 1992; Ravanel *et al*., 2001).

Bacterial strains were a *K. pneumoniae* laboratory strain and isogenic mutants (Benghezal *et al*., 2006), the isogenic *P. aeruginosa* strains PT5 and PT531 (*rhlR-lasR* avirulent mutant) (Cosson *et al*., 2002), the *P. aeruginosa* strain PT894 and the isogenic DP5 (*trpD*) and DP28 (*pchH*) avirulent mutants (Alibaud *et al*., 2008), the *E. coli* strains DH5α (Invitrogen), and B/r (Gerisch, 1959), non-sporulating *B. subtilis* 36.1 (Ratner and Newell, 1978), *Micrococcus luteus* (Wilczynska and Fisher, 1994), and the avirulent *Aeromonas salmonicida* JF2397 strain (Froquet *et al*., 2007).

Cell culture and mutagenesis

Dictyostelium discoideum cells were grown at 21°C in HL5 medium (Mercanti *et al*., 2006) and subcultured twice a week to maintain a density $< 10^6$ cells ml^{-1}.

To test the effect of various ions on growth of *Dictyostelium*, cells were cultivated in HL5 complemented with increasing concentrations of various ions, to attain a concentration at which growth was slowed down but not fully inhibited ($MgCl_2$: 100 mM, KCl: 200 mM, NaCl. 150 mM, $CaCl_2$: 80 mM, $MnCl_2$: 15 mM, $CdCl_2$: 50 μM, $NiCl_2$: 350 μM). Growth curves were obtained in these conditions by seeding the cells at 10 000 cells ml^{-1} and recording their growth over up to 3 weeks.

To isolate killing-deficient mutants, cells were mutagenized by restriction enzyme-mediated integration of the pSC plasmid (Cornillon *et al*., 2000; Guerin and Larochelle, 2002), and transfected cells selected in the presence of blasticidin (10 μg ml^{-1}). A cell sorter was used to clone single cells into individual wells of 96-wells plates. A Replica Plater for 96 wells plate (Sigma-Aldrich) was used to transfer 2 μl of each clone to a lawn of *Klebsiella*. Overall, 2000 individual clones were tested for their ability to grow efficiently on *Klebsiella* and five were unable to. Mutant cells were expanded and their genomic DNA was extracted. The inserted pSC plasmid was recovered with the genomic flanking regions after a ClaI digestion and the insertion site determined by sequencing (Cornillon *et al*., 2000). Further studies were focused on one of these clones (*kil2*), which was the only one corresponding to an insertion within a coding sequence. A new knockout vector was constructed to delete the sequence of the *kil2* gene (Figs 1C and S1). Transfected cells were cloned by limiting dilution, and screened by PCR (Fig. S1) (Charette and

Cosson, 2004). Two independent mutant clones were used with identical results in all experiments presented in this study.

Growth of Dictyostelium *on bacteria*

Procedures to test growth of various *Dictyostelium* strains on bacteria have been described previously (Froquet *et al*., 2009). Briefly, bacteria were grown overnight in LB, then 50 µl of the culture was deposited and dried on 2 ml of SM-Agar (10 g l^{-1} peptone, 1 g l^{-1} yeast extract, 2.2 g l^{-1} KH_2PO_4, 1 g l^{-1} K_2HPO_4, 1 g l^{-1} $MgSO_4$:$7H_2O$, 10 g l^{-1} glucose, 20 g l^{-1} Agar) in one well of a 24-well plate. When indicated, an antibiotic was added to the SM-agar (gentamycin 25 µg ml^{-1}) or bacteria were boiled at 95°C during 4 h before depositing them on SM-Agar. Variable numbers of wild-type or mutant *Dictyostelium* amoebae (10 000, 1000, 100 or 10) were deposited on the bacterial lawn, and allowed to grow at 21°C for 4–5 days, i.e. until individual colonies of wild-type *Dictyostelium* became visible.

Intracellular killing of bacteria by Dictyostelium

Phagocytosis and killing of bacteria were assessed as described previously (Benghezal *et al*., 2006). Briefly, 1.5×10^4 bacteria from an overnight liquid culture (in LB for *Klebsiella* or *B. subtilis*; in SM deprived of glucose for *P. aeruginosa* PT531) were mixed with 10^6 *Dictyostelium* cells in 500 µl of phosphate buffer (2 mM Na_2HPO_4, 14.7 mM KH_2PO_4, pH 6.5) and incubated at 21°C with shaking. When indicated, salts were added to the phosphate buffer: $MgCl_2$ (10 mM), $CaCl_2$ (10 mM), NaCl (10 mM), KCl (10 mM), $MnCl_2$ (10 µM), $FeSO_4$ (10 µM) or $ZnCl_2$ (1 µM) or $NiCl_2$ (0.5 µM). After 0, 1, 2, 4 or 6 h of incubation, a 10 µl aliquot of the suspension was collected, diluted in 40 µl of ice-cold sucrose (400 g l^{-1}). Two hundred microlitre phosphate buffer containing 0.5% saponin was added, before plating on a LB-agar plate and incubating at 37°C. This procedure was previously shown to kill *Dictyostelium* cells, without affecting bacterial viability. The bacterial colonies were counted 24 h later. When indicated, the number of viable bacteria associated with *Dictyostelium* cells (intracellular fraction) was determined by washing the cells twice with ice-cold HL5 medium before diluting in sucrose.

In order to visualize live intracellular bacteria, 25×10^6 GFP-expressing *Klebsiella* from an overnight culture were mixed with 5×10^5 *Dictyostelium* cells in 500 µl of HL5 medium. After 60 min of shaking incubation, cells were allowed to attach on a glass coverslip for 30 min, fixed and processed for immunofluorescence as described previously (Mercanti *et al*., 2006) using the H161 monoclonal antibody and an Alexa-546-coupled secondary antibody to reveal the endosomal p80 marker. Cells were analysed with a LSM510 confocal microscope (Carl Zeiss).

Intracellular replication of *Mycobacterium* was determined as described (Hagedorn and Soldati, 2007), *Dictyostelium* cells were incubated with *M. marinum* expressing GFP and the replication of bacteria was followed during 2 days using a flow cytometer. When cells were analysed by confocal microscopy, they were fixed and the p80 marker revealed by immunofluorescence.

Purification of phagosomes

Phagosomes containing latex beads were purified as described (Gotthardt *et al*., 2006b). Briefly, *Dictyostelium* cells were incubated with 0.8 µm latex beads during a pulse of 5 or 15 min, then washed and incubated further for 15 or 45 min. Phagosomes containing latex beads were purified by flotation on sucrose gradient. Proteins were then separated in SDS-polyacrylamide gels, transferred to nitrocellulose, detected with specific antibodies, horseradish-peroxidase-coupled secondary antibodies (Bio-Rad), and visualized by ECL.

Endosomal and lysosomal pathways

Endosomal pH was measured as described in (Marchetti *et al*., 2009), by following at various times after internalization the fluorescence levels of two internalized dextrans, one coupled to a pH-sensitive fluorophore (Oregon green), and one to a pH-insensitive fluorophore (Alexa 647). Lysosomes and post-lysosomes were detected by co-immunofluorescence with antibodies to H^+-ATPase and p80, and their number and size analysed as previously described (Charette and Cosson, 2007). Transfer of internalized latex beads from lysosomes to post-lysosomes was measured as described previously (Charette and Cosson, 2007) to determine the rates of transfer between these two compartments. Briefly, *Dictyostelium* cells were incubated 15 min with FITC-latex beads, washed to eliminate uningested beads, and then incubated for different times before fixation and immunofluorescence. The number of beads in lysosomes (H^+-ATPase-positive, p80-positive) and post-lysosomes (H^+-ATPase-negative, p80-positive) was determined, and the fraction present in post-lysosomes is indicated.

The activity of lysosomal enzymes in cells and in the extracellular medium was measured using a colorimetric assay as described previously (Froquet *et al*., 2008).

Kinetic analysis of phagosomal proteolytic activity was performed using a fluorescence plate reader (Synergy Mx, Biotek) as described (Russell *et al*., 2009), based on the principle of dye dequenching induced by proteolysis of the carrier protein. Briefly, the proteolytic reporter Self-Quenched BODIPY® Dye Conjugates of Bovine Serum Albumin (DQ Green BSA, Molecular Probes) was coupled to 3 µm carboxylate-modified silica particles (Kisker Biotech). As a reference dye, particles were also coupled with Alexa Fluor 594-SE (Molecular Probes). *Dictyostelium* cells were plated as a monolayer in clear bottom black wall 96-well dishes (Costar) and allowed to adhere in phosphate buffer. The fluorescent beads were added to the cells at a ratio of 1:2 and the plate was centrifuged for 30 s. Non-ingested beads were removed immediately by washing twice with phosphate buffer supplemented, when indicated with 10 mM $MgCl_2$. The emission fluorescence was measured in the same buffer at 490 nm and 450 nm excitation every 90 s over a period of 180 min. The 490/450 nm ratio reflects the bulk proteolytic activity within the bead-containing phagosomes.

Acknowledgements

This work was supported by grants from the Fonds National Suisse de la Recherche Scientifique (http://www.snf.ch) to P.C. and T.S. The P.C. research group is supported by the Doerenkamp-Zbinden Foundation (http://www.doerenkamp.ch) and the Fondation E. Naef pour la Recherche in Vitro (http://www.fondation-naef.com). The P.C. and T.S. research groups are part of the NEMO network supported by the 3R Research Foun-

dation Switzerland (http://www.forschung3r.ch). We thank Drs Brian VanderVen and David G. Russell for the opportunity to learn the proteolytic activity assay in their lab, supported by an 'Individual short visit fellowship' to MH (Swiss National Science Foundation IZK0A3-121674). We thank S.J. Charette (Université Laval, Canada) for critical reading of the manuscript.

References

Alibaud, L., Kohler, T., Coudray, A., Prigent-Combaret, C., Bergeret, E., Perrin, J., *et al*. (2008) *Pseudomonas aeruginosa* virulence genes identified in a *Dictyostelium* host model. *Cell Microbiol* **10:** 729–740.

Alix, E., and Blanc-Potard, A.B. (2007) MgtC: a key player in intramacrophage survival. *Trends Microbiol* **15:** 252–256.

Appelberg, R. (2006) Macrophage nutriprive antimicrobial mechanisms. *J Leukoc Biol* **79:** 1117–1128.

Axelsen, K.B., and Palmgren, M.G. (1998) Evolution of substrate specificities in the P-type ATPase superfamily. *J Mol Evol* **46:** 84–101.

Benghezal, M., Fauvarque, M.O., Tournebize, R., Froquet, R., Marchetti, A., Bergeret, E., *et al*. (2006) Specific host genes required for the killing of *Klebsiella* bacteria by phagocytes. *Cell Microbiol* **8:** 139–148.

Caterina, M.J., Milne, J.L., and Devreotes, P.N. (1994) Mutation of the third intracellular loop of the cAMP receptor, cAR1, of *Dictyostelium* yields mutants impaired in multiple signaling pathways. *J Biol Chem* **269:** 1523–1532.

Catty, P., de Kerchove d'Exaerde, A., and Goffeau, A. (1997) The complete inventory of the yeast *Saccharomyces cerevisiae* P-type transport ATPases. *FEBS Lett* **409:** 325–332.

Charette, S.J., and Cosson, P. (2004) Preparation of genomic DNA from *Dictyostelium* discoideum for PCR analysis. *Biotechniques* **36:** 574–575.

Charette, S.J., and Cosson, P. (2007) A LYST/beige homolog is involved in biogenesis of *Dictyostelium* secretory lysosomes. *J Cell Sci* **120:** 2338–2343.

Cornillon, S., Pech, E., Benghezal, M., Ravanel, K., Gaynor, E., Letourneur, F., *et al*. (2000) Phg1p is a nine-transmembrane protein superfamily member involved in dictyostelium adhesion and phagocytosis. *J Biol Chem* **275:** 34287–34292.

Cosson, P., and Soldati, T. (2008) Eat, kill or die: when amoeba meets bacteria. *Curr Opin Microbiol* **11:** 271–276.

Cosson, P., Zulianello, L., Join-Lambert, O., Faurisson, F., Gebbie, L., Benghezal, M., *et al*. (2002) *Pseudomonas aeruginosa* virulence analyzed in a *Dictyostelium* discoideum host system. *J Bacteriol* **184:** 3027–3033.

Cronin, S.R., Rao, R., and Hampton, R.Y. (2002) Cod1p/Spf1p is a P-type ATPase involved in ER function and Ca2+ homeostasis. *J Cell Biol* **157:** 1017–1028.

Dieckmann, R., Gopaldass, N., Escalera, C., and Soldati, T. (2008) Monitoring time-dependent maturation changes in purified phagosomes from *Dictyostelium* discoideum. *Methods Mol Biol* **445:** 327–337.

Eichinger, L., Pachebat, J.A., Glockner, G., Rajandream, M.A., Sucgang, R., Berriman, M., *et al*. (2005) The genome of the social amoeba *Dictyostelium* discoideum. *Nature* **435:** 43–57.

Froquet, R., Cherix, N., Burr, S.E., Frey, J., Vilches, S., Tomas, J.M., and Cosson, P. (2007) Alternative host model to evaluate *Aeromonas* virulence. *Appl Environ Microbiol* **73:** 5657–5659.

Froquet, R., Cherix, N., Birke, R., Benghezal, M., Cameroni, E., Letourneur, F., *et al*. (2008) Control of cellular physiology by TM9 proteins in yeast and *Dictyostelium*. *J Biol Chem* **283:** 6764–6772.

Froquet, R., Lelong, E., Marchetti, A., and Cosson, P. (2009) *Dictyostelium* discoideum: a model host to measure bacterial virulence. *Nat Protoc* **4:** 25–30.

Garcia Vescovi, E., Soncini, F.C., and Groisman, E.A. (1996) Mg2+ as an extracellular signal: environmental regulation of Salmonella virulence. *Cell* **84:** 165–174.

Garin, J., Diez, R., Kieffer, S., Dermine, J.F., Duclos, S., Gagnon, E., *et al*. (2001) The phagosome proteome: insight into phagosome functions. *J Cell Biol* **152:** 165–180.

Gerisch, G. (1959) Ein submerskulturverfahren für entwicklungsphysiologische untersuchungen an *Dictyostelium* discoideum. *Naturwissenschaften* **46:** 654–656.

Gitler, A.D., Chesi, A., Geddie, M.L., Strathearn, K.E., Hamamichi, S., Hill, K.J., *et al*. (2009) Alpha-synuclein is part of a diverse and highly conserved interaction network that includes PARK9 and manganese toxicity. *Nat Genet* **41:** 308–315.

Gotthardt, D., Blancheteau, V., Bosserhoff, A., Ruppert, T., Delorenzi, M., and Soldati, T. (2006a) Proteomics fingerprinting of phagosome maturation and evidence for the role of a Galpha during uptake. *Mol Cell Proteomics* **5:** 2228–2243.

Gotthardt, D., Dieckmann, R., Blancheteau, V., Kistler, C., Reichardt, F., and Soldati, T. (2006b) Preparation of intact, highly purified phagosomes from *Dictyostelium*. *Methods Mol Biol* **346:** 439–448.

Guerin, N.A., and Larochelle, D.A. (2002) A user's guide to restriction enzyme-mediated integration in *Dictyostelium*. *J Muscle Res Cell Motil* **23:** 597–604.

Haas, A. (2007) The phagosome: compartment with a license to kill. *Traffic* **8:** 311–330.

Hagedorn, M., and Soldati, T. (2007) Flotillin and RacH modulate the intracellular immunity of *Dictyostelium* to *Mycobacterium marinum* infection. *Cell Microbiol* **9:** 2716–2733.

Marchetti, A., Lelong, E., and Cosson, P. (2009) A measure of endosomal pH by flow cytometry in *Dictyostelium*. *BMC Res Notes* **2:** 7.

Martin-Orozco, N., Touret, N., Zaharik, M.L., Park, E., Kopelman, R., Miller, S., *et al*. (2006) Visualization of vacuolar acidification-induced transcription of genes of pathogens inside macrophages. *Mol Biol Cell* **17:** 498–510.

Mercanti, V., Charette, S.J., Bennett, N., Ryckewaert, J.J., Letourneur, F., and Cosson, P. (2006) Selective membrane exclusion in phagocytic and macropinocytic cups. *J Cell Sci* **119:** 4079–4087.

Neuhaus, E.M., Almers, W., and Soldati, T. (2002) Morphology and dynamics of the endocytic pathway in *Dictyostelium* discoideum. *Mol Biol Cell* **13:** 1390–1407.

Papp-Wallace, K.M., and Maguire, M.E. (2006) Manganese transport and the role of manganese in virulence. *Annu Rev Microbiol* **60:** 187–209.

Peracino, B., Wagner, C., Balest, A., Balbo, A., Pergolizzi, B., Noegel, A.A., *et al*. (2006) Function and mechanism of action of *Dictyostelium* Nramp1 (Slc11a1) in bacterial infection. *Traffic* **7:** 22–38.

Ramirez, A., Heimbach, A., Grundemann, J., Stiller, B., Hampshire, D., Cid, L.P., *et al*. (2006) Hereditary parkinsonism with dementia is caused by mutations in ATP13A2, encoding a lysosomal type 5 P-type ATPase. *Nat Genet* **38:** 1184–1191.

Ratner, D.I., and Newell, P.C. (1978) Linkage analysis in *Dictyostelium* discoideum using multiply marked tester strains: establishment of linkage group VII and the reassessment of earlier linkage data. *J Gen Microbiol* **109:** 225–236.

Ravanel, K., de Chassey, B., Cornillon, S., Benghezal, M., Zulianello, L., Gebbie, L., *et al*. (2001) Membrane sorting in the endocytic and phagocytic pathway of *Dictyostelium* discoideum. *Eur J Cell Biol* **80:** 754–764.

Reeves, E.P., Lu, H., Jacobs, H.L., Messina, C.G., Bolsover, S., Gabella, G., *et al*. (2002) Killing activity of neutrophils is mediated through activation of proteases by K+ flux. *Nature* **416:** 291–297.

Russell, D.G., Vanderven, B.C., Glennie, S., Mwandumba, H., and Heyderman, R.S. (2009) The macrophage marches on its phagosome: dynamic assays of phagosome function. *Nat Rev Immunol* **9:** 594–600.

Schmidt, K., Wolfe, D.M., Stiller, B., and Pearce, D.A. (2009) Cd2+, Mn2+, Ni2+ and Se2+ toxicity to *Saccharomyces cerevisiae* lacking YPK9p the orthologue of human ATP13A2. *Biochem Biophys Res Commun* **383:** 198–202.

Schultheis, P.J., Hagen, T.T., O'Toole, K.K., Tachibana, A., Burke, C.R., McGill, D.L., *et al*. (2004) Characterization of the P5 subfamily of P-type transport ATPases in mice. *Biochem Biophys Res Commun* **323:** 731–738.

Segal, A.W. (2005) How neutrophils kill microbes. *Annu Rev Immunol* **23:** 197–223.

Sumimoto, H., Miyano, K., and Takeya, R. (2005) Molecular composition and regulation of the Nox family NAD(P)H oxidases. *Biochem Biophys Res Commun* **338:** 677–686.

Troll, H., Malchow, D., Muller-Taubenberger, A., Humbel, B., Lottspeich, F., Ecke, M., *et al*. (1992) Purification, functional characterization, and cDNA sequencing of mitochondrial porin from *Dictyostelium* discoideum. *J Biol Chem* **267:** 21072–21079.

Underhill, D.M., and Ozinsky, A. (2002) Phagocytosis of microbes: complexity in action. *Annu Rev Immunol* **20:** 825–852.

Wilczynska, Z., and Fisher, P.R. (1994) Analysis of a complex plasmid insertion in a phototaxis-deficient transformant of *Dictyostelium* discoideum selected on a Micrococcus luteus lawn. *Plasmid* **32:** 182–194.

Supporting information

Additional Supporting Information may be found in the online version of this article:

Fig. S1. Isolation of *kil2* knockout mutants. A. Schematic representation of the *kil2* gene in wild-type or *kil2* cells and of the *kil2* knockout vector. Arrows indicate the position of oligonucleotides used to construct the knockout vector and to identify knockout mutant cells. B. Sequences of the oligonucleotides and their position on the *kil2* genomic sequence are indicated. C. *kil2* knockout mutants were identified by PCR with three different pairs of oligonucleotides. The PCR fragment observed after amplification of wild-type genomic DNA with pairs 1 + 4 and 5 + 6 is absent when *kil2* mutant cells are tested. In *kil2* mutant cells, a specific PCR amplification is seen with oligonucleotides 1 + BSRa. The results obtained with wild-type cells and three independent *kil2* knockout clones are shown.

Fig. S2. Phylogenetic tree of P-type ATPases in five eukaryotic organisms. Protein sequences of P-type ATPases from five fully sequenced eukaryotic genomes were aligned with CLUSTALX 2.0 program. The distance-based phylogenetic tree was generated using the neighbour-joining algorithm (as implemented in the PHYLIP package), and bootstrap assessment of the tree topology was performed with one thousand replicates. The branch lengths are proportional to the number of amino acid substitutions per site. Numbers at the nodes represent percentage of bootstrap support (only values > 60% are indicated). Uniprot protein IDs are shown, followed by the organism abbreviation: *D. discoideum* (DI), *H. sapiens* (HU), *A. thaliana* (AT), *S. cerevisiae* (YST) and *S. pombe* (SPO). Kil2 clusters with P-type ATPases from group V (Axelsen and Palmgren, 1998).

Fig. S3. The endosomal pH is very similar in wild-type and *kil2* cells. Endosomal pH was measured in wild-type and *kil2* mutant cells following a protocol described previously (Marchetti *et al*., 2009). For this, *Dictyostelium* cells were incubated for 20 min in the presence of a mixture of dextran coupled to Oregon green- (OG, pH-sensitive) and to Alexa 647 (A-647, pH-insensitive). The cells were then washed and incubated further in HL5. The intracellular fluorescence was measured by flow cytometry at each indicated time. This experiment was repeated three times with equivalent results. A. The cell-associated fluorescence of both probes exhibited the same profiles in wild-type and *kil2* cells. B. The fluorescence ratio of the two probes provides an estimate of the pH of endosomes at various times following endocytosis. The endosomal pH is virtually identical at all times in wild-type and *kil2* mutant cells. C. A calibration curve was obtained in parallel by incubating cells having endocytosed dextrans in medium at a defined pH, in the presence of sodium azide and ammonium chloride. Approximate pH values can be obtained by comparing the values in B with the calibration curve. These results demonstrate that in wild-type and *kil2* cells, fluid phase is endocytosed, transferred from acidic lysosomes to less acidic post-lysosomes, and recycled to the extracellular medium with virtually identical kinetics. It also indicates that the pH of the various endocytic compartments is indistinguishable in both cell types.

Fig. S4. The general organization of the endocytic/phagocytic pathway is not altered in *kil2* mutant cells. A. In order to measure the kinetics of maturation of phagosomes, *Dictyostelium* cells were incubated with 1 μm latex beads for 15 min, washed to eliminate non-internalized beads and incubated further for 15, 45 and 75 min (total incubation time of 30, 60 and 90 min). Cells were then fixed, and p80 and H^+-ATPase were detected by immunofluorescence in order to determine if beads were present in lysosomes (p80-positive, H^+-ATPase-positive) or post-lysosomes (p80-positive, H^+-ATPase-negative). At each time, 30 internalized beads were analysed, and the percentage of beads present in post-lysosomes was determined. The average and SEM of three independent experiments are indicated. In wild-type and in *kil2* cells, all internalized beads were

found initially in lysosomes, then transferred with very similar kinetics to post-lysosomes. B. Cells were grown for 3 days in HL5 medium, and recovered by centrifugation. The activity of two lysosomal enzymes (NAG: N-acetyl β-glucosaminidase; MAN: α-mannosidase) was determined in cell pellets and in supernatants. The total activity of lysosomal enzymes (full bars) was similar in wild-type and *kil2* mutant cells. In both cells, only a small fraction of lysosomal enzymes was released in the medium (empty bars). Each bar indicates the average and SEM of three independent experiments.

Fig. S5. *Mycobacterium marinum* replicates normally in *kil2* mutant cells. *Dictyostelium* cells were infected with wild-type or mutant (L1D) *M. marinum* expressing GFP (green). A. At 37 h post-infection, cells were fixed and p80 revealed by immunofluorescence (white). *Mycobacterium* replication vacuoles were indistinguishable in wild-type and *kil2* cells: several bacteria were found within p80-positive replication vacuoles (upper panel) from which they also escaped into the cytosol (lower panel) (scale bar: 5 μm). B. Intracellular replication of *M. marinum* was measured by flow cytometry over a period of 2 days. The total amount of fluorescence (intracellular and extracellular) is indicated. Wild-type *M. marinum* replicated with similar kinetics in *kil2* and in wild-type cells. L1D mutant mycobacteria were incapable of replicating in either cell type.

Fig. S6. *nramp1* mutant cells kill *Klebsiella* efficiently. Wild-type or *nramp1* cells were incubated with *Klebsiella* and the number of remaining live bacteria was determined at different times by plating an aliquot on LB plates and counting bacterial colony forming units, as described in the legend to Fig. 5. Wild-type and *nramp1* mutant cells killed *Klebsiella* with very similar kinetics.

Table S1. Endocytic compartments are very similar in wild-type and *kil2* cells. Endocytic compartments were analysed by confocal microscopy in wild-type or *kil2* cells: endosomal p80 and H^+-ATPase were detected by immunofluorescence in order to differentiate lysosomes (Ly, p80-positive, H^+-ATPase-positive) and post-lysosomes (PL, p80-positive, H^+-ATPase-negative). Compartments were counted, and their size determined in at least 20 cells. The average and SEM values in three independent experiments are indicated.

Please note: Wiley-Blackwell are not responsible for the content or functionality of any supporting materials supplied by the authors. Any queries (other than missing material) should be directed to the corresponding author for the article.